Aromatic and Antiaromatic Pathways in Triphyrin(2.1.1) Annelated with Benzo[b]heterocycles

Bartkowski, Krzysztof

2019-12-05

Bartkowski , K , Dimitroya , M , Chmielewski , P J , Sundholm , D & Pawlicki , M 2019 , ' Aromatic and Antiaromatic Pathways in Triphyrin(2.1.1) Annelated with Benzo[b]heterocycles ' , Chemistry: A European Journal , vol. 25 , no. 68 , pp. 15477-15482 . https://doi.org/10.1002/chem.201903863

http://hdl.handle.net/10138/319461
https://doi.org/10.1002/chem.201903863

unspecified
acceptedVersion

Aromatic and Antiaromatic Pathways in Triphyrin(2.1.1) Annelated with Benzo[*b*]heterocycles

Krzysztof Bartkowski,[a] Maria Dimitrova,[b] Piotr J. Chmielewski,[a] Dage Sundholm[b] and Miłosz Pawlicki*[a]

Abstract: *Understanding of the aromatic properties and magnetically induced current densities of highly conjugated chromophores is important when designing molecules with strongly delocalised electronic structure. Linear extension of the triphyrin(2.1.1) skeleton with an annelated benzo[b]heterocycle fragment modifies the aromatic character by extending the electron delocalisation pathway. Two-electron reduction leads to an antiaromatic triphyrin(2.1.1) ring and an aromatic benzo[b]heterocycle subunit. Current-density calculations provide detailed information about the observed pathways and their strengths.*

Extending the π-electron system in conjugated molecules is an important area of research, because the conjugation pathway exhibits notable influence on the optical and magnetic properties.[1] Linear extensions of the acene π cloud by annelation of molecular rings lead to different aromatic behaviour of five- and six-membered rings.[3,4] A side fusion of a five-membered ring to acene cores results in major differences in the electron delocalisation with the bridging heteroatom separating the aromatic and antiaromatic moieties.[5]

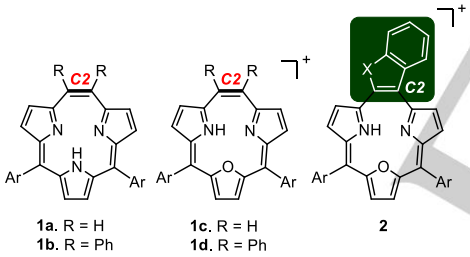

Scheme 1. The molecular structure of triphyrins(2.1.1). The green box encloses the benzo[*b*]heterocycle subunit.

Triphyrins(2.1.1) (Scheme 1) are triangularly shaped, contracted porphyrinoids whose structural constraints significantly affect their electronic properties.[2] The C2 bridge (**1**, Scheme 1) makes it possible to merge an acene to the triphyrin macrocycle potentially resulting in molecular structures with novel optical and magnetic properties as well as an unusual aromatic character.[2d,2e]

We have synthesized novel molecular structures with benzo[*b*]furan and benzo[*b*]thiophene annelated to triphyrin(2.1.1) (**2**, Scheme 1). The annelated arene ring may influence the global aromatic properties by incorporating the external benzoic (C6) ring into the delocalisation pathway. The synthesized macrocycles can also function as boron(III) ligands forming antiaromatic complexes as shown in this work.

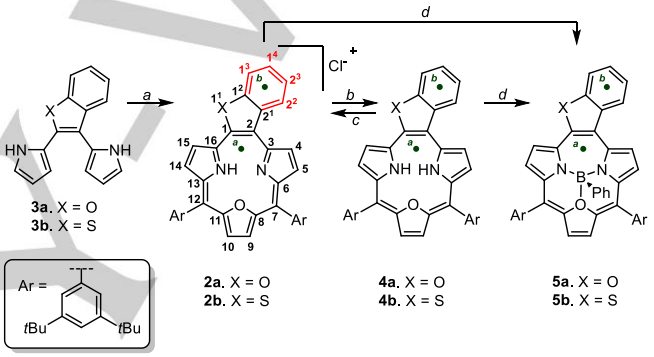

Scheme 2. Synthetic approach. Conditions: a) 1. 2,5-bis(3,5-di-*t*-butylphenyl)furan, CH_2Cl_2, BF_3Et_2O, 2. DDQ, 3. Anion exchange; b) Zn/Hg (excess), $CH(D)Cl_3$, argon; c) air; d) $PhBCl_2$ toluene, Et_3N, argon, reflux).

Triphyrins **2a** and **2b** were obtained by acid-catalysed condensation of reagents **3a** and **3b,** respectively. They were efficiently synthesized via Suzuki-Miyaura coupling from easily obtainable and commercially available starting materials (2,3-dibromobenzo[*b*]heterocycle and pyrrole-boronic acid),[6] followed by a thermolytic deprotection.[2d,2e] **2a** and **2b** were isolated with a yield of 10% and 12%, respectively. The small coordination core of the macrocycle leads to a very efficient entrapment of a proton making it possible to isolate the cationic form. As the counterion of the condensation product was unknown, we replaced it with a chloride anion by using a previously reported approach.[2d,2e] Characterization and further studies were performed on the chloride derivatives.

2a (**2b**) has a UV-Vis spectrum that is typical for aromatic porphyrinoids with a Soret-like band at 415 nm (430 nm) and a set of Q bands that reach 600 nm (620 nm). The bands are red shifted by 40-50 nm as compared to triphyrins(2.1.1) such as **1b**[2b] and **1c**[2f], whose electron delocalisation pathway is limited to 14 π electrons. The red shift suggests that the annelated C6 fragment is part of the π–electron delocalisation. Triphyrin **2a** (**2b**) fluoresces at 615 nm (640 nm) with a Stokes shift of ~20 nm. The fluorescence quantum yield is 0.12 (0.01). The S_1 lifetime (τ_1) of 2.6 ns (0.6 ns) contributes $4.6\cdot10^7$ s^{-1}/$3.4\cdot10^8$ s^{-1} ($1.7\cdot10^7\cdot s^{-1}$/$17\cdot10^8$ s^{-1}) to the radiative/non-radiative (k_r/k_{nr}) rate constants. The

[a] K. Bartkowski, Prof. P. J. Chmielewski, Dr M. Pawlicki
Department of Chemistry, University of Wrocław
F. Joliot-Curie 14, 50383 Wrocław, POLAND
E-mail: milosz.pawlicki@chem.uni.wroc.pl
www: http://mjplab.org

[b] M. Dimitrova, Prof. D. Sundholm
University of Helsinki, Department of Chemistry, Faculty of Science, P.O. Box 55, FIN-00014 University of Helsinki, Finland
email: dage.sundholm@helsinki.fi

Supporting information for this article is given via a link at the end of the document.((Please delete this text if not appropriate))

excitation spectrum recorded at 615 nm (640 nm) (Figure S36-S37) confirms the origin of the observed fluorescence.

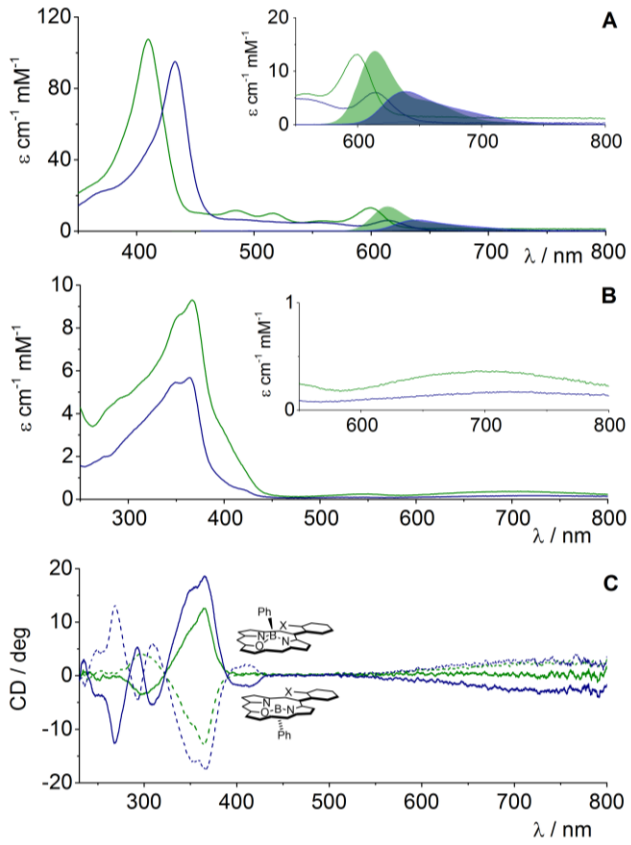

Figure 1. The absorption and emission spectra of **2a** (green) and **2b** (blue) (A) and the absorption spectra of **5a** (green) and **5b** (blue) (B) measured in CH_2Cl_2 at 295 K. CD experiments (C) performed for **5a** (green) and **5b** (blue) (CH_2Cl_2, 295 K).

Triphyrin **2a** (**2b**) can be reversibly reduced. The electrochemical experiments (Figure S38-39) yielded two well-resolved reductions at –664 mV (–668 mV) and –1136 mV (–1123 mV) relatively to the ferrocene (Fc/Fc+) pair in dichloromethane. No oxidation was registered for the whole tested region of 0 – (+)1.8 V. The redox modifications significantly change the aromatic character. **2a** (**2b**) is reduced to **4a** (**4b**) by treating it with an excess of a zinc amalgam in an inert atmosphere (Scheme 1, path b). The absorption spectrum of **4a** (**4b**), significantly different from that of **2a** (**2b**). **4a** (**4b**) is air sensitive and exposure to ambient conditions quantitatively converts it to the starting reagents. **4a** (**4b**) can entrap boron(III) cation yielding **5a** (**5b**) complexes, which was synthesized by a two-step reaction of **2a** (**2b**) with phenylboron(III) dichloride in boiling toluene in the presence of triethyl amine as reducing agent (Scheme 2, d). The complexes can also be obtained via a consecutive reduction and insertion process.[2d,e,7] The aromatic character of **5a** (**5b**) differs from that of **2a** (**2b**), since the shape of the absorption spectra (Figure 1B) is characteristic for antiaromatic porphyrinoids with 4n π electrons.[1,2d,e,7] **5a** (**5b**) have intense Soret-like bands at 370 nm (365 nm) accompanied bands are very broad red-shifted transitions with small oscillator strengths. **5a** (**5b**) does not fluoresce, which is typical for antiaromatic molecules.[8,9] **5a** (**5b**) is chiral, belonging to the non-symmetric C_1 point group. The chirality was documented by measured the Cotton effect for **5a** (**5b)** enantiomers with identical UV-Vis and NMR spectra using a chiral column (Figure 1C). The absolute configurations of the **5a** (**5b**) enantiomers were assigned by comparing experimental CD spectra with spectra calculated at the time-dependent density functional theory (TDDFT) level. The calculated and measured spectra qualitatively agree (see SI).

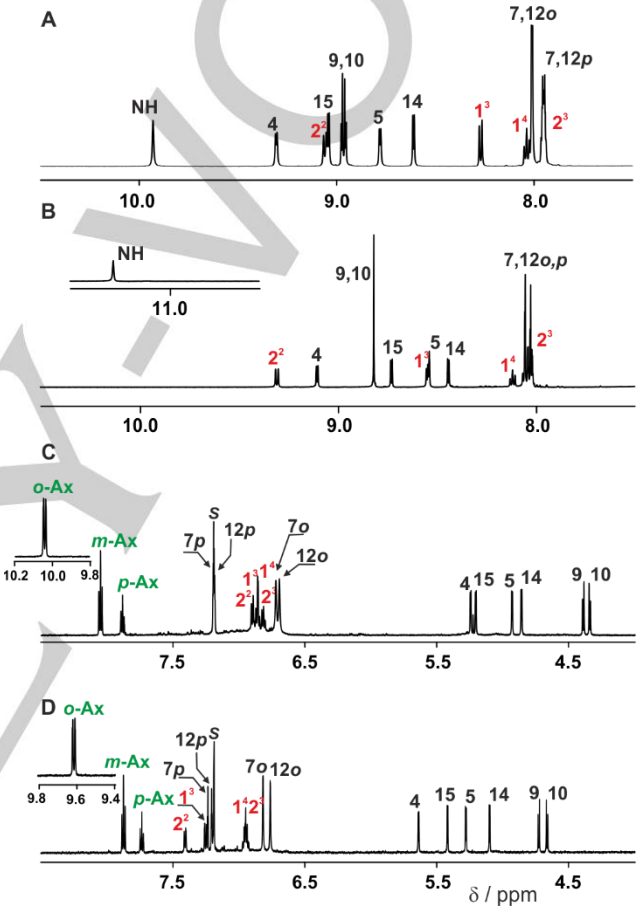

Figure 2. The 1H NMR spectra of **2a** (A), **2b** (B), **5a** (C) and **5b** (D) measured in chloroform-*d*, (600 MHz, 300 K).

The aromatic character is analysed based on the measured ^{1}H NMR spectra. The cations appear to be aromatic (Figure 2A, B), since all resonances assigned to the perimeter of the macrocycle are significantly downfield shifted (**2a** δ = 9.31 ppm (4), δ = 8.78 ppm (5), δ =8.95 ppm (9), δ = 8.98 ppm (10), δ = 8.61 ppm (14), δ = 9.04 ppm (15) and for **2b** δ = 9.08 ppm (4), δ = 8.54 ppm (5), δ = 8.84 ppm (9,10), δ = 8.43 ppm (14), δ = 8.73 ppm (15)) suggesting that the macrocycle sustains a global diatropic ring current, which is also expected to shift the ^{1}H NMR signal of the inner entrapped hydrogen upfield, [1,14] However, the inner hydrogen of **2a** (**2b**) has a significant downfield shift of δ = 9.98 ppm (δ = 11.35 ppm) in the ^{1}H NMR spectrum as shown in Figure

2. The ^{1}H NMR spectrum for **4a** (**4b**) shows upfield relocation of the perimeter lines to the region of δ = 5.2-6.2 ppm (Figure S18 and Figure S22) with the two NH resonances shifted to δ = 19.1 ppm (17.3 ppm) and δ = 17.1 ppm (14.5 ppm) for **4a** (**4b**) suggesting a change of the aromatic character from aromatic to antiaromatic.[1] Significantly more upfield shifted signals were recorded for the boron(III) complexes (**5a** δ = 5.29 ppm (4), δ = 4.98 ppm (5), δ = 4.45 ppm (9), δ = 4.39 ppm (10), δ = 5.26 ppm (14), δ = 4.91 ppm (15) and for **5b** δ = 5.69 ppm (4), δ = 5.33 ppm (5), δ = 4.78 ppm (9), δ = 4.71 ppm (10), δ = 5.15 ppm (14), δ = 5.47 ppm (15)), which is typical for antiaromatic porphyrinoids.[1,7] The chemical shifts of the axial aryl group attached to the central boron inside the macrocycle are sensitive probes for assessing the aromatic character of the macrocycle.[1,10] The significantly downfield shifted resonances of the axial phenyl group (Figure 2C,D; **5a** δ = 10.09 ppm *ortho*, δ = 8.08 ppm *meta*, δ = 7.93 ppm *para*; **5b** δ = 9.66 ppm *ortho*, δ = 7.92 ppm *meta*, δ = 7.78 ppm *para*) confirm that the macrocycle is antiaromatic. The antiaromatic character is also supported by the measured UV-Vis spectra (Figure 1).

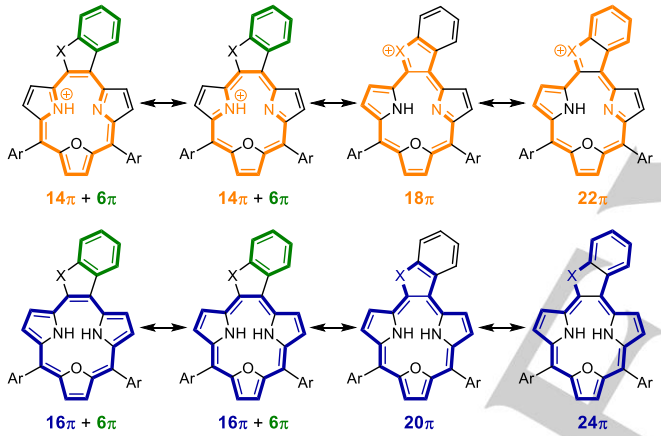

Scheme 3. Resonance equilibria for oxidized (top) and reduced (bottom) forms of triphyrin(2.1.1) annelated with benzo[b]heterocycles.

The spectroscopic analysis suggests that the electron delocalisation of the oxidized (aromatic) and reduced (antiaromatic) triphyrins cannot be described with a single aromatic pathway. The aromatic pathway may consist of several routes (Scheme 3) that include the annelated fragment (18/22 π for aromatic and 20/24 π for antiaromatic) or solely following the internal circuit (14+6 π or 16+6 π respectively). The absorption and emission spectra suggest a significant contribution to the aromatic character from an extended delocalisation in the aromatic structures, and from only the inner pathway in the antiaromatic triphyrins. ^{1}H NMR chemical shifts are very sensitive probes for assessing the degree of aromaticity.[1] The protons at positions 1^3, 1^4, 2^2 and 2^3 (Scheme 2) in the acyclic **3a** (**3b**) → aromatic **2a** (**2b**) → antiaromatic **4a** (**4b**) compounds suggest that the annelated C6 ring plays different roles for the current-density pathways in the aromatic and antiaromatic triphyrins. With the starting structures **3a** (**3b**) as a reference, significant differences in the ^{1}H NMR chemical shifts of the C6 hydrogens are observed. In the aromatic **2a** (**2b**), the C6 resonances at 8.2-9.2 ppm (Figure 2) are strongly downfield shifted, suggesting an extension of delocalisation over the annelated fragment and a substantial contribution from the 22 π-electron resonance structure. Two electron reduction and formation of **4a** (**4b**) brings the C6 resonances at 7.1-7.0 ppm (7.5-7.1 ppm) close to the signal positions of 7.5-7.2 ppm (7.7-7.3 ppm) for **3a** (**3b**), which suggests that the delocalisation of the C6 fragment is isolated from the current density pathway of the macroring, which leads to the presence of both aromatic and antiaromatic character in the same molecule. The annelated C6 ring with 6π electrons is aromatic and the triphyrin ring is antiaromatic with 16 π electrons in the antiaromatic pathway (Scheme 3). The aromatic and antiaromatic character is even more prominent in the boron(III) complexes **5a** (**5b**).

Molecular structure optimisations and calculations of the magnetically induced current densities (MICD),[16] nucleus independent chemical shifts (NICS),[12] the anisotropy of the induced current density (AICD),[15] were performed as described in the SI. Calculated NICS values, AICD plots, the NMR chemical shifts relative to tetramethylsilane (TMS), and the optimised coordinates of the molecular structures are given as SI.

The calculations show that the positively charged **2a** (**2b**) is almost planar, whereas the molecular structure of **4a** (**4b**) is significantly distorted from planarity. The insertion of phenylboron(III) yielding **5a** (**5b**) leads to a more planar structure than for **4a** (**4b**) as also suggested by the spectroscopic studies (Figure 3). The calculated NICS(1) value of –11.80 ppm (–11.60 ppm) in point a of **2a** (**2b**) shows that it is aromatic. The two-electron reduction yields the antiaromatic **4a** (**4b**) with a NICS value of +13.4 ppm, (+11.87 ppm) in point a. The boron(III) complex **5a** (**5b**) is more antiaromatic than **4a** with a NICS value of +18.94 ppm (+11.60 ppm) in point a. The NICS(1) value of +11.60 ppm for **4b** is practically the same as for **2b**. The annelated C6 ring of **2a** and **4a** (**2b** and **4b**) are aromatic with NICS(1) values of –11.18 ppm and –11.17 ppm (–10.69 ppm and–11.05 ppm) in point b. The AICD plots in the SI show that the diatropic current in **2a** (**2b**) splits into two pathways with the stronger ring current along the 22π electron pathway (Figure S42). The AICD analysis of the reduced **4a** (**4b**) and **5a** (**5b**) molecules (Figure S43-44) suggests that there is an antiaromatic 16π electron pathway in the main macrocycle and that the 6π electrons of the annelated C6 ring sustain a diatropic ring current. The AICD plots suggest that **4a** (**4b**) and **5a** (**5b**) sustain diatropic and paratropic ring currents. The paratropic ring current of the 16π delocalisation pathway passes the inner pyrrole nitrogens, whereas the C=C bridges are not part of the aromatic pathway of **4a** (**4b**) and **5a** (**5b**)

The more detailed GIMIC[16] analyses of the MICD confirm that **2a** (**2b**) sustains net diatropic ring current of 23.4 nA/T (21.8 nA/T) around the macroring, which is comparable to the ring-current strength of 27 nA/T for the free-base porphyrin.[17] The main part of the global ring current of **2a** (**2b**) passes around the C6 ring. The strength of the current density flowing via the outer pathway at the C6 ring is 13.8 nA/T (14.2 nA/T). The C6 ring in **2a** sustains a weak local ring current of 2.1 nA/T, whereas the C6 ring of **2b** does not sustain any local ring current. The pathway of the global ring current of **2b** splits into a stronger branch passing

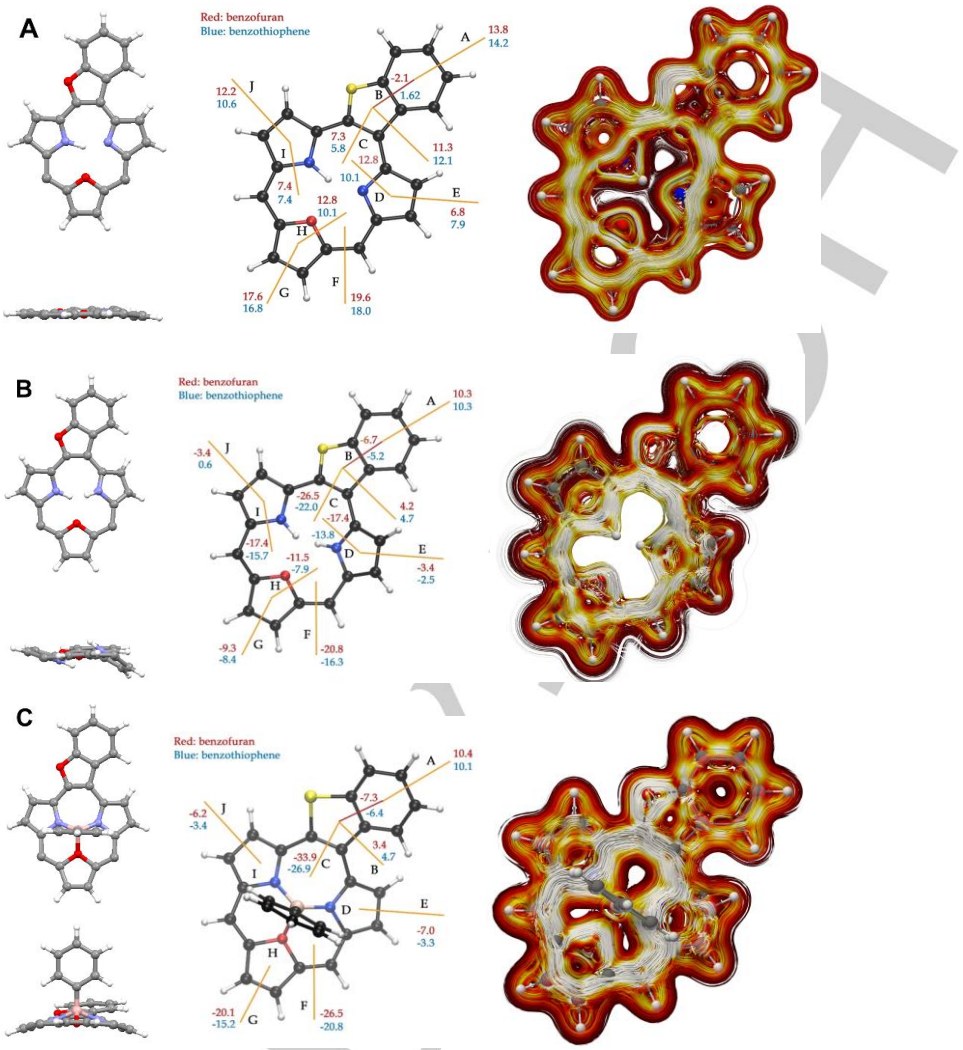

Figure 3. The optimized molecular structures, the strengths of current pathways, and MICD plot for **2a** (A), **4a** (B) and **5a** (C). The integrated current strengths (in nA/T) passing selected chemical bonds of **2a** (**2b**), **4a** (**4b**), and **5a** (**5b**) are given in red (blue). Current strengths of the most important current pathways are reported in Table S1 in the SI. The molecular pictures to the right show the most relevant current pathways of **2a** (**2b**), **4a** (**4b**), and **5a** (**5b**).

on the outside of the C6 ring, and a weak branch of 1.6 nA/T passing between the thiophene and C6 rings. The current strength of the pathway between the benzofuran (benzothiophene) moiety and the triphyrin(2.1.1) ring is 7.3 nA/T (5.8 nA/T).

The MICD calculations show that **4a** (**4b**) is antiaromatic with the macroring sustaining a net paratropic ring currents of -20.8 nA/T (-16.3 nA/T), which is comparable to the ring-current strength of -25 nA/T for doubly oxidized octaethylporphyrinate zinc(II).[18] The current density in **4a** (**4b**) is more complex than for **2a** (**2b**) and consists of diatropic and paratropic contributions with a global diatropic ring current of about 3.4 nA/T (3.8 nA/T) that flows along the outer contour of the entire molecule. The observed antiaromatic character originates from the strong paratropic ring current flowing mainly along the inner pathway of the macroring. Figure 3 shows that the paratropic ring current splits in two branches at the furan ring, which is typical for porphyrinoids.[17,19] The atomic current at the nitrogen moiety of the pyrrolic rings forces the global paratropic ring current on the inner side of the heteroatom. In contrast, at the furan ring of the macroring, the current density splits via the inner and outer pathway between the nitrogen atom and the C–C bond with about the same strength. Benzofuran in **4a** and benzothiophene in **4b** sustain a weak diatropic ring current of 4.2 nA/T (4.7 nA/T). A local diatropic ring current of 6.7 nA/T (5.2 nA/T) is sustained by the C6 ring. For **4a** and **4b**, the strength of the ring current passing the outer part of the C6 ring is 10.3 nA/T, which is close to the net ring-current strength of 11.8 nA/T for benzene.[20] The neutral boron-containing complex **5a** (**5b**) is antiaromatic sustaining a strong net paratropic ring current of -26.5 nA/T (-20.8 nA/T). The ring-current pathways of **5a** (**5b**) and **4a** (**4b**) are very similar.

However, the detailed analysis of the current pathways is more difficult for **5a** (**5b**) than for **4a** (**4b**) due to the interference of the phenyl substituent of the boron. The current strength of the two branches at the pyrrolic rings were estimated by rotating the

phenyl group by 90 degrees before integration, since the global ring-current strength was found to be almost independent of the orientation of the phenyl substituent. The local diatropic current density at the nitrogen moiety of the pyrrolic ring forces the paratropic ring current inwards as in **4a** (**4b**). The net strength of the ring current passing the outer part of the C6 ring of **5a** (**5b**) is 10.4 nA/T (10.1 nA/T). The C6 ring sustains a local diatropic ring current of about 10 nA/T (9 nA/T) that extends along the C–C bond between the C6 and the triphyrin rings, where it turns back to the common C–C bond of the C6 ring and the furan (thiophene) ring. (Figure 3).

We have shown that molecules consisting of benzo[*b*]furan and benzo[*b*]thiophene annelated to triphyrin(2.1.1) skeletons lead to two strongly aromatic molecules with about two thirds of the ring current passing along the 22π–electron pathway on the outer side of the annelated C6 motif. The rest of the diatropic ring current takes the 18π–electron pathway. The current pathways have been determined spectroscopically as well as by employing NICS, AICD and MICD calculations. Quantitative values for the ring-current strength along possible ring-current pathways have been obtained by integrating the MICD passing selected bonds.
The aromatic character can be modified by reduction, which leads to molecules that sustain diatropic ring currents in the benzo[*b*]furan and benzo[*b*]thiophene moieties and paratropic ring currents around the triphyrin(2.1.1) ring. The paratropic ring current of the 16π-electron inner pathway is slightly stronger for the boron(III) complexes, where the phenylboron unit preserves the antiaromatic character of the triphyrin ring and the aromaticity of the benzo[b]heterocycle fragment. The asymmetric character of the boron(III) complexes results in a rare planar chirality of the antiaromatic molecules.[13] We are pursuing further experiments on the delocalization control of acene-triphyrin(2.1.1) hybrids.

Acknowledgements

Financial support from the National Science Centre, Poland (2015/17/B/ST5/01437) and the Academy of Finland (1314821), Magnus Ehrnrooth Foundation, and the Finnish Cultural Foundation is kindly acknowledged. The Wrocław Supercomputer Centre (KDM WCSS (MP)), CSC – the Finnish IT Center for Science and the Finnish Grid and Cloud Infrastructure (persistent identifier urn:nbn:fi:researchinfras-2016072533) are acknowledged for computer time.

Keywords: triphyrin • aromaticity • antiaromaticity • chirality • acenes

[1] M. Pawlicki, L. Latos-Grażyński, *Chem. Asian J.* **2015**, *10*, 1438-1451.

[2] a) Z.-L. Xue, Z. Shen, J. Mack, D. Kuzuhara, H. Yamada, T. Okujima, N. Ono, X.-Z. You, N. Kobayashi, *J. Am. Chem. Soc.* **2008**, *130*, 16478–16479; b) K. S. Anju, S. Ramakrishnan, A. Srinivasan, *Org. Lett.* **2011**, *13*, 2498–2501; c) D. Kuzuhara, Y. Sakakibara, S. Mori, T. Okujima, H. Uno, H. Yamada, *Angew. Chem. Int. Ed.* **2013**, *52*, 3360–3363; d) M. Pawlicki, K. Hurej, L. Szterenberg, L. Latos-Grażyński *Angew. Chem. Int. Ed.* **2014**, *53*, 2992-2996; e) M. Pawlicki, M. Garbicz, L. Szterenberg, L. Latos-Grażyński *Angew. Chem. Int. Ed.* **2015**, *54*, 1906-1909, f) D. Kuzuhara, S. Kawatsu, W. Furukawa, H. Hayashi, N. Aratani, H. Yamada *Eur. J. Org. Chem.* **2018**, 2122-2129; g) A. Kumar, K. Thorat, M. Ravikanth, *Org. Lett.* **2018**, *20*, 4871-4874; h) K. N. Panda, K. G. Thorat, M. Ravikanth, *J. Org. Chem.* **2018**, *83*, 12945-12950; i) J. Klajn, W. Stawski, J. Cybińska, P.J. Chmielewski, M. Pawlicki, *Chem. Commun.* **2019**, *55*, 4558-4561.

[3] J. E. Anthony *Chem. Rev.* **2006**, *106*, 5028-5048.

[4] C. K. Frederickson, B. D. Rose, M. M. Haley, *Acc. Chem. Res.* **2017**, *50*, 977-987.

[5] a) J. L. Marshall, K. Uchida, C. K. Frederockson, Ch. Schutt, A. M. Zeidell, K. P. Goetz, T. W. Finn, K. Jarolimek, L. N. Zakharov, C. Risko, R. Herges, O. D. Jurchescu, M. M. Haley, *Chem. Sci.*, **2016**, *7*, 5547-5558; b) R. E. Messersmith, S. Yadav, M. A. Siegler, H. Ottosson, J. D. Tovar, *J. Org. Chem.*, **2017**, *82*, 13440–13448.

[6] R. Liu, Ch. von Malotki, L. Arnold, N. Koshino, H. Higashimura, M. Baumgarten, K. Mullen *J. Am. Chem. Soc.* **2011**, *133*, 10372-10375.

[7] T. Kakui, S. Sugawara, Y. Hirata, S. Kojima, Y. Yamamoto, *Chem. Eur. J.* **2011**, *17*, 7768–7771

[8] a) S. Cho, Z. S. Yoon, K. S. Kim, M.-C. Yoon, D.-G. Cho, J. L. Sessler, D. Kim, *J. Phys. Chem. Lett.* **2010**, *1*, 895–900; b) M. S. Yamaguchi, B. S. Lee, Y. M. Sung, S. Kuhri, C. A. Schierl, D. M. Guldi, D. Kim, Y. Matsuo, *J. Am. Chem. Soc.* **2012**, *134*, 16540–16543.

[9] a) M. Pawlicki, K. Hurej, K. Kwiecińska, L. Szterenberg, L. Latos-Grażyński, *Chem. Commun.* **2015**, *51*, 11362-11365; b) K. Hurej, W. Stawski, L. Latos-Grażyński, M. Pawlicki *Chem. Asian. J.* **2016**, *11*, 3329-3333.

[10] a) J. A. Cissell, T. P. Vaid, G. P. A. Yap, *J. Am. Chem. Soc.* **2007**, *129*, 7841–7847; b) J. A. Cissell, T. P. Vaid, A. G. DiPasquale, A. L. Rheingold, *Inorg. Chem.* **2007**, *46*, 7713–7715, c) A. Młodzianowska, L. Latos-Grażyński, L. Szterenberg, M. Stępień *Inorg. Chem.* **2007**, *46*, 6950-6957; d) A. Idec, M. Pawlicki, L. Latos-Grażyński, *Inorg. Chem.* **2017**, *56*, 10337-10352, e) M. Pawlicki, A. Kędzia, D. Bykowski, L. Latos-Grażyński, *Chem. Eur. J.* **2014**, *20*, 17500-17506.

[11] a) M. Pawlicki, A. Kędzia, L. Szterenberg, L. Latos-Grażyński *Eur. J. Org. Chem.* **2013**, 2770-2774.

[12] Z. Chen, C. S. Wannere, C. Corminboeuf, R. Puchta, P. von. R. Schleyer, *Chem. Rev.*, **2005**, *105*, 3842–3888.

[13] a) X. Fu, Y. Meng, X. Li, M. Stępień, P. J. Chmielewski *Chem. Commun.* **2018**, *54*, 2510-2513; b) A. Idec, M. Pawlicki, L. Latos-Grażyński, *Chem. Eur. J.* **2019**, *25*, 250-254.

[14] a) I. C. Calder, F. Sondheimer *Chem. Commun. (London)*, **1966**, 904-905; b) E. L. Spitler, C. A. Johnson II, M. M. Haley *Chem. Rev.*, **2006**, *106*, 5344-5386; c) C. D. Stevenson, T. L. Kurth *J. Am. Chem. Soc.* **2000**, *122*, 722-723.

[15] a) R. Herges, D. Geuenich *J. Phys. Chem. A* **2001**, *105*, 3214-3220; b) D. Geuenich, K. Hess, F. Köhler, R. Herges *Chem. Rev.* **2005**, *105*, 3758.

[16] D. Sundholm, H. Fliegl, R. J. F. Berger *WIREs Comput. Mol. Sci.* **2016**, *6*, 639–678.

[17] H. Fliegl, D. Sundholm, *J. Org. Chem.* **2012**, *77*, 3408-3414.

[18] H. Fliegl, F. Pichierri, D. Sundholm, *J. Phys. Chem. A* **2015**, *119*, 2344-2350.

[19] a) H. Fliegl, D. Sundholm, S. Taubert, F. Pichierri, *J. Phys. Chem. A* **2010**, *114*, 7153-7161; b) H. Fliegl, D. Sundholm, F. Pichierri, *Phys. Chem. Chem. Phys.* **2011**, *13*, 20659-20665; c) H. Fliegl, N. Özcan, R. Mera-Adasme, F. Pichierri, J. Jusélius, D. Sundholm, *Mol. Phys.* **2013**, *111*, 1364-1372; d) R. R. Valiev, H. Fliegl, D. Sundholm, *J. Phys. Chem. A* **2013**, *117*, 9062-9068; e) R. R. Valiev, H. Fliegl, D. Sundholm, *J. Phys. Chem. A* **2015**, *119*, 1201-1207; f) R. R. Valiev, H. Fliegl, D. Sundholm, *Phys. Chem. Chem. Phys.* **2014**, *16*, 11010-11016; g) H. Fliegl, R. R. Valiev, F. Pichierri, D. Sundholm, *Chem. Modell.* **2018**, *14*, 1-42.

[20] H. Fliegl, D. Sundholm, S. Taubert, J. Jusélius, W. Klopper, *J. Phys. Chem. A* **2009**, *113*, 8668-8676.

Entry for the Table of Contents (Please choose one layout)

COMMUNICATION

Aromaticity Fusion! Annelation of a benzo[*b*]heterocycle subunit to the C2 bridge of triphyrin(2.1.1) significantly modifies its aromatic character. Two-electron reduction changes the aromaticity from global aromatic to antiaromatic delocalisation in the triphyrin(2.1.1) ring, whereas the benzo[*b*]heterocycle moiety remains aromatic.

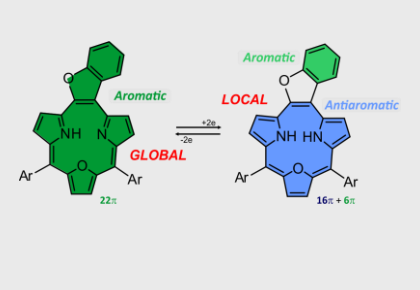

*Krzysztof Bartkowski, Maria Dimitrova, Piotr J. Chmielewski, Dage Sundholm and Miłosz Pawlicki**

Page No. – Page No.

Aromatic and Antiaromatic Pathways in Triphyrin(2.1.1) Annelated with Benzo[*b*]heterocycles